

Determination of the Axial Correlation Lengths and Paracrystalline Distortion for Aromatic Copolyimides of Random Monomer Sequence

Tzong-Ming Wu, John Blackwell,* and Sergei N. Chvalun†

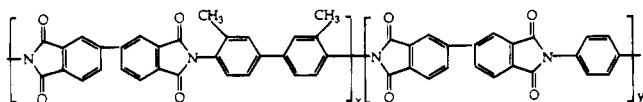
Department of Macromolecular Science, Case Western Reserve University, Cleveland, Ohio 44106-7202

Received May 8, 1995; Revised Manuscript Received August 4, 1995*

ABSTRACT: X-ray methods have been used to investigate the structure of aromatic copolyimide fibers prepared from 3,3',4,4'-biphenyltetracarboxylic dianhydride (BPDA), *o*-tolidine (OTOL), and *p*-phenylenediamine (PPD). The X-ray fiber diagrams of these copolymers contain nonperiodic layer lines that are indicative of a random comonomer sequence. The meridional peak positions are reproduced accurately in the predicted scattering for an infinite chain with random sequence and highly extended chain conformation. However, there is a less than adequate match between the observed and calculated peak profiles, which are predicted to be very much sharper than those observed. It is shown that the latter match is improved by consideration of chains of finite length with significant distortions from linearity. The results favor a sinuous chain conformation consisting of highly but not completely extended segments separated by less ordered regions or discontinuities. From analysis of the peak profiles, we have derived the correlation length in the chain axis direction, analogous to the axial crystallite size for homopolymers. This correlation length is 180 Å for homopoly(BPDA–OTOL) but increases steadily with the introduction of PPD comonomer, reaching approximately 1000 Å for the 60/40 BPDA–OTOL/BPDA–PPD copolymer at a $\times 12$ draw ratio. The results are compared to those for Kevlar 149 poly(*p*-phenylene terephthalamide) fibers, for which the observed axial crystallite width is 395 Å, much less than for the copolyimides. The correlation length and sinuosity are independent of OTOL/PPD ratio at constant draw ratio. Hence the increasing linearity obtained at higher PPD content and higher draw ratio is simply due to the presence of the more flexible BPDA–PPD units.

Introduction

This paper describes further X-ray analysis of the structure of fibers of the aromatic copolyimides prepared by condensation reaction of 3,3',4,4'-biphenyltetracarboxylic dianhydride (BPDA) with mixtures of *o*-tolidine (OTOL) and *p*-phenylenediamine (PPD). The chemical structure of copoly(BPDA–OTOL/BPDA–PPD) is shown below; the chemical compositions (*x*/*y*) studied in the present work are 100/0, 80/20, 70/30, and 60/40.



Incorporation of the PPD monomer leads to increases in both drawability and thermal stability when compared to homopoly(BPDA–OTOL)¹ and to tensile properties that are comparable to those for Kevlar 49 polyaramid fibers.² We have reported previously that the X-ray fiber diagrams of these copolyimides contain nonperiodic layer lines that are characteristic of random microstructure.³ Excellent agreement was obtained between the observed axial *d*-spacings and those predicted for extended chains of completely random comonomer sequence. Modification of the combination statistics to consider nonrandom sequences eliminated this agreement, and all but minimal nonrandomness could be ruled out.

We also observed that some of the nonperiodic meridional maxima sharpen with increasing draw ratio

and also shift to slightly lower scattering angles (i.e., higher Bragg *d*-spacings).⁴ It was shown that these observations are to be understood primarily in terms of an increase in the extended chain correlation length for the random sequences. This is analogous to an increase in crystallite size for homopolymers, which leads to a sharpening of the Bragg reflections and can also result in small changes in *d*-spacing: the peaks in the Laue function for the lattice can shift slightly when multiplied by the more slowly varying Fourier transform of the unit cell contents.

The correlation length for the extended chain conformation was derived from the width (along the fiber axis direction) of the sharp meridional maximum on the 4th layer line, which becomes progressively sharper with increasing PPD content. We showed that part of this line broadening is due to the random microstructure but that there is additional broadening due to the finite correlation length for the extended chain, which led to estimates of the latter for different comonomer ratios and draw ratios. The results pointed to a conformation consisting of highly extended rodlike segments separated by less ordered regions or “discontinuities”. The length of the rodlike segments was found to increase with PPD content, and it was suggested that the absence of the methyl substituent groups lowers the barrier for torsional rotation about the *N*-phenyl bond and facilitates adoption of a more linear conformation during the drawing process.

As also pointed out in our earlier paper,⁴ this analysis tended to underestimate the length of the ordered regions because we assumed these contain perfectly straight chains, whereas all stereochemically acceptable models for even the most highly extended chains have a sinuous character. Such sinuosity is analogous to one-dimensional paracrystallinity in the structure of a homopolymer chain. In the present paper we have

* To whom correspondence should be addressed. Tel. (216) 368-4172; FAX (216) 368-4202; E-mail jxb6@po.cwru.edu.

† Present address: Karpov Institute of Physical Chemistry, 103064 Moscow, ul. Vorontzovo Pole 10, Russia.

* Abstract published in *Advance ACS Abstracts*, September 15, 1995.

extended our analyses to include the effect of chain sinuosity in order to obtain more accurate estimates of the correlation length in the ordered regions of the extended copolymer chains. It will be seen below that the extended chain correlation lengths derived for the copolymers are considerably greater than that measured for Kevlar 149 fibers.

Experimental Section

The homopoly(BPDA-OTOL) and copoly(BPDA-OTOL/BPDA-PPD) fibers were prepared in the laboratory of Professors S. Z. D. Cheng and F. W. Harris at the University of Akron and were those described previously in our joint publication.⁴ Homopoly(BPDA-OTOL) was synthesized from BPDA and OTOL in *p*-chlorophenyl at 210 °C under reflux for 6 h and showed an intrinsic viscosity of 9.3 dL/g in *p*-chlorophenyl at 60 °C. The copolymers were prepared from mixtures of BPDA, OTOL, and PPD in *p*-chlorophenyl solution at OTOL/PPD molar ratios of 80/20, 70/30, and 60/40, which were heated under reflux at 210 °C for 6 h. The water liberated by the polycondensation was removed by distillation. Fibers of the homopolymer and copolymers were prepared from isotropic solution by dry-jet wet spinning into a coagulation bath of water/methanol, and these were then drawn in air in the range of 440–480 °C.^{1,5} In the work described below, we studied specimens prepared at their maximum draw ratios (λ): $\lambda = 2$ for the homopolymer and $\lambda = 5, 8$, and 12 for the 80/20, 70/30, and 60/40 copolymers, respectively. We also compared specimens of all three copolymers at the same draw ratio, $\lambda = 5$.

X-ray Diffraction. Specimens for X-ray diffraction were prepared as parallel bundles of about 15–20 fibers. Linear $\theta/2\theta$ X-ray intensity scans of the fibers along the meridional (fiber axis) direction were recorded using Cu K α radiation and a Philips PN 3550/10 diffractometer equipped with a diffracted beam monochromator. The instrument was used in the transmission mode with a constant slit of 0.03°. These data were recorded at 0.02° increments of 2θ for the 4th and 8th layer lines and at 0.05° increments of 2θ for the 12th layer line. The measurement time at each angular increment was sufficient for ~2000 counts at the center of each peak. Silicon powder with a 325 mesh size was used as a standard sample to evaluate the instrumental broadening, for which we assumed Gaussian profiles. A linear background correction was applied separately to each of the three observed peaks before curve fitting to obtain the integral half-widths.

Molecular Models

Atomic coordinates for the monomer residues were based on bond lengths, bond angles and torsion angles derived from the model compound pyromellitic dianhydride–oxydianiline⁶ and from standard data bases. Molecular models for the homopolymer chains were constructed using the SYBYL software package (Tripos Inc.). The minimum energy conformations matched the observed fiber repeats derived from the X-ray data for the homopolymers. For the predictions of the scattering of the random copolyimides along the fiber axis direction, we used models with axial advances of 20.43 Å for BPDA-OTOL and 15.78 Å for BPDA-PPD. These are the repeats for minimum energy conformations for the two homopolymers, for which the observed repeats are 20.43 ± 0.02 Å for homopoly(BPDA-OTOL) and 15.79 ± 0.02 Å for homopoly(BPDA-PPD).^{3,7}

Data Analysis

Line Broadening for Homopolymers. The observed integral half-width for an hkl reflection, δ , can be separated into two components via

$$\delta^2 = \delta_c^2 + \delta_\beta^2 \quad (1)$$

where δ_c and δ_β are the contributions due to finite crystallite size and distortions (paracrystallinity), respectively.⁸ The crystallite size perpendicular to the hkl lattice plane, L_{hkl} , is given by the Scherrer equation:

$$L_{hkl} = 1/\delta_c \quad (2)$$

L_{hkl} is in angstroms when δ_c is measured in s units ($s = 2 \sin \theta/\lambda$, where θ is half the scattering angle and λ is the wavelength in angstroms). δ_β is given by

$$\delta_\beta = (1 - H_1(Z))/2d_{hkl} \quad (3)$$

where $H_1(Z)$ is the Fourier transform of the distribution function for d_{hkl} , the mean interplane spacing. If this distribution is modeled by a Gaussian function, for the series of orders of hkl (hkl ; $2h, 2k, 2l$; etc.)

$$\delta_\beta = (1 - \exp(-2\pi^2 g^2 n^2))/2d_{hkl} \quad (4)$$

where g is the standard deviation expressed as a fraction of d_{hkl} , and n is the order. When $2\pi^2 g^2 n^2$ is much smaller than the unity, the numerator in eq 4 can be approximated as $2\pi^2 g^2 n^2$, such that

$$\delta^2 = 1/L_{hkl}^2 + (\pi g n)^4/d_{hkl}^2 \quad (5)$$

A plot of δ^2 versus n^4 has intercept $1/L_{hkl}^2$ and slope $(\pi g)^4/d_{hkl}^2$, leading to estimates of L_{hkl} and g .

Scattering by Extended Chains of Random Copolymers. The present copolyimides can be thought of as sequences of two monomers A and B, i.e., BPDA-OTOL and BPDA-PPD. Prediction of the scattering by random copolymers with extended chain conformation^{9–14} used concepts that are similar to those in the treatment of paracrystallinity in homopolymers. $H_1(Z)$ is the Fourier transform of the first nearest-neighbor terms in the autocorrelation function $Q(z)$ of an extended chain. When there is constant axial advance for each monomer,

$$H_1(Z) = \sum_A \sum_B p_A p_B F_{AB}(Z) \exp(2\pi i Z z_B) \quad (6)$$

where p_A and p_B are the molar fractions of monomers A and B, z_B is the axial advance for monomer B, and $F_{AB}(Z)$ is the Fourier transform of the cross convolution of monomer A with monomer B, given by

$$F_{AB}(Z) = \sum_{j=1}^{N_A} \sum_{k=1}^{N_B} f_{A,j} f_{B,k} \exp(2\pi i Z (z_{B,k} - z_{A,j})) \quad (7)$$

The subscripts A,j and B,k designate the j th of N_A atoms of monomer A and the k th of N_B atoms of monomer B, respectively. If the chain is sinuous, such that the monomer axial advances are only approximately constant, it is necessary to replace $\exp(2\pi i Z z_B)$ ($=X_B$) in eq 6 by a distribution function. If this distribution is assumed to be Gaussian with standard deviation σ , X_B becomes

$$X_B = \exp(-2\sigma^2 \pi^2 Z^2) \exp(2\pi i Z z_B) \quad (8)$$

$I(Z)$, the intensity along the z axis direction for an infinite chain, is given by

$$I(Z) = \text{Re} \left(\frac{1 + H_1(Z)}{1 - H_1(Z)} \right) \quad (9)$$

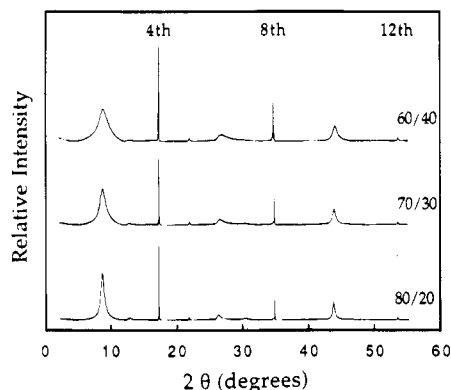


Figure 1. Calculated intensity along the chain axis direction for idealized infinite straight chains of 80/20, 70/30, and 60/40 copoly(BPDA-OTOL/BPDA-PPD).

Table 1. Observed and Calculated Integral Half-Widths (in deg) of the 4th, 8th, and 12th Layer Line Intensity Maxima for the 80/20, 70/30, and 60/40 Copolymers

	draw ratio (λ)	observed	infinite straight chain	finite sinuous chain
80/20	5			$N = 25, \sigma = 0.164 \text{ \AA}$
4th		0.247 ± 0.006	0.057	0.247
8th		0.423 ± 0.009	0.224	0.425
12th		0.82 ± 0.02	0.43	0.81
70/30	8			$N = 42, \sigma = 0.152 \text{ \AA}$
4th		0.189 ± 0.004	0.075	0.189
8th		0.381 ± 0.008	0.295	0.385
12th		0.79 ± 0.02	0.68	0.78
60/40	12			$N = 55, \sigma = 0.133 \text{ \AA}$
4th		0.186 ± 0.004	0.095	0.184
8th		0.336 ± 0.007	0.324	0.346
12th		0.74 ± 0.02	0.73	0.76
70/30	5			$N = 27, \sigma = 0.158 \text{ \AA}$
4th		0.260 ± 0.006	0.075	0.261
8th		0.436 ± 0.009	0.295	0.439
12th		0.84 ± 0.02	0.68	0.83
60/40	5			$N = 29, \sigma = 0.148 \text{ \AA}$
4th		0.281 ± 0.007	0.095	0.281
8th		0.447 ± 0.009	0.324	0.451
12th		0.85 ± 0.02	0.73	0.84

where Re designates the real components. For a finite chain of N monomers, this becomes

$$I(Z) = \text{Re} \left(\left(\frac{1 + H_1(Z)}{1 - H_1(Z)} \right) - \left(\frac{H_1(Z)(1 - H_1^N(Z))}{N(1 - H_1(Z))^2} \right) \right) \quad (10)$$

For an infinite chain model with constant axial advances for the two monomers, the peaks in $I(Z)$ are nonperiodic and, in general, have finite width. The only exceptions are some of the peaks predicted for chains in which z_A and z_B are simple multiples of a common length factor, a ; for example, $z_A = 3a$ and $z_B = 4a$. In such a case, we predict periodic δ -functions at $Z = 1/a, 2/a, 3/a$, etc., with broader, aperiodic peaks between them. The periodic peaks are invariant; i.e., their positions are independent of monomer ratio. For a finite and/or sinuous chain, the sharp maxima are broadened, and thus their widths in the observed data can be used to evaluate the length and sinuosity of the scattering units, in the same way as we derive the crystallite size and paracrystallinity index for a homopolymer. From eqs 6–10, the calculated peak profiles depend on chemical composition through p_A and p_B , the chain length through N , and the distribution of axial projection lengths through σ .

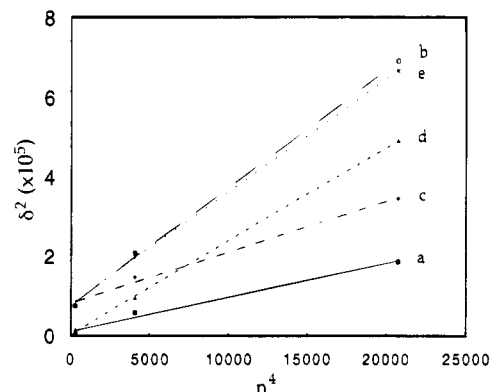


Figure 2. Plots of observed and calculated δ^2 against n^4 for the 80/20 copolymer ($\lambda = 5$): (a) calculated for an infinite straight chain; (b) observed data; (c) calculated for a finite straight chain: $N = 20$, length = 390 Å; (d) calculated for an infinite chain with sinuosity: $\sigma = 0.166 \text{ \AA}$, $g = 0.85\%$; (e) calculated for a finite, sinuous chain: $N = 25$, length = 480 Å, $\sigma = 0.164 \text{ \AA}$, $g = 0.84\%$.

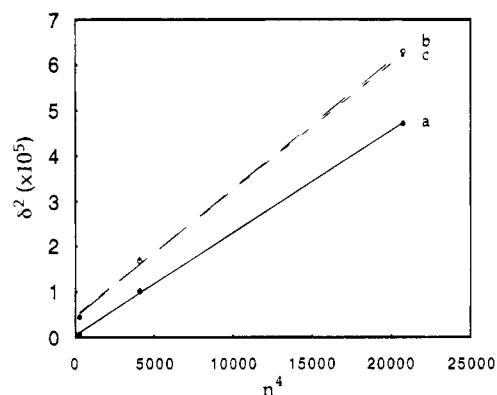


Figure 3. Plots of observed and calculated δ^2 against n^4 for the 70/30 copolymer ($\lambda = 8$): (a) calculated for an infinite straight chain; (b) observed data; (c) calculated for a finite, sinuous chain: $N = 42$, length = 800 Å, $\sigma = 0.152 \text{ \AA}$, $g = 0.80\%$.

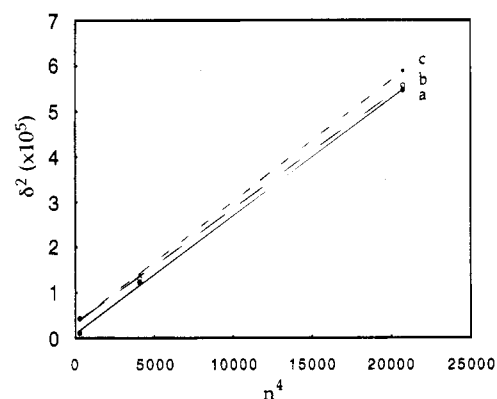


Figure 4. Plots of observed and calculated δ^2 against n^4 for the 60/40 copolymer ($\lambda = 12$): (a) calculated for an infinite straight chain; (b) observed data; (c) calculated for a finite, sinuous chain: $N = 55$, length = 1000 Å, $\sigma = 0.133 \text{ \AA}$, $g = 0.72\%$.

The peak widths in $I(Z)$ were determined by the same method used for the observed data. The calculated intensity was plotted against 2θ , and the integral half-widths were determined by fitting Gaussian functions to the 4th-, 8th-, and 12th-order peaks. For the 4th and 8th orders, the intensity falls to essentially zero on either side of the peaks. However, this is not the case for the 12th order, and a linear background drawn between the minima on either side of the peak was subtracted before fitting a Gaussian function.

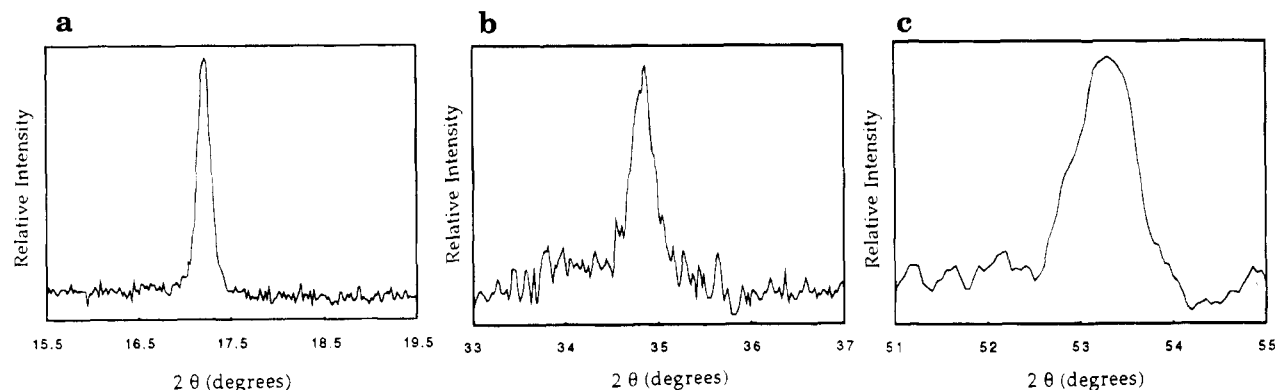


Figure 5. Observed intensity profiles along the chain axis direction on the (a) 4th, (b) 8th, and (c) 12th layer lines for fibers of 70/30 copoly(BPDA-OTOL/BPDA-PPD) at a draw ratio of $\lambda = 8$.

Results and Discussion

Figure 1 shows the calculated $I(Z)$ for the 80/20, 70/30, and 60/40 copolymers, based on idealized infinite straight chain models with BPDA-OTOL and BPDA-PPD advances equal to the monomer lengths: 20.43 and 15.78 Å, respectively. It is seen that these data contain relatively strong, sharp maxima on the 4th-, 8th-, and 12th-layer lines, which are the first three orders of a repeat of ~ 5.2 Å. These peaks arise because of the approximate coincidence of the 4th order of 20.43 Å and the 3rd order of 15.78 Å. There is not an exact coincidence, and hence the predicted peaks are not δ -functions but have finite widths (δ), which are listed in Table 1. Plots of δ^2 against n^4 for these calculated data are shown in Figures 2, 3, and 4 (curve a in each case) for the 80/20, 70/30, and 60/40 copolymers, respectively. In each case we obtained an approximate straight line plot with a positive slope. This is to be expected since the prediction of $I(Z)$ in eq 9 is similar to that used for a one-dimensional paracrystalline homopolymer structure.⁸ The fit to a straight line is not perfect, in that the second point is generally above and the first and third are generally below the best straight lines. But even for a paracrystalline homopolymer the treatment is only an approximation, and there are additional complexities due to the cross-terms in the calculation of $I(Z)$ for the two-component system. Nevertheless, the intercept at $n^4 = 0$ is very close to the origin, consistent with the infinite chain model (i.e., analogous to infinite crystal size).

Figure 5 shows the observed $I(Z)$ data for the 4th-, 8th-, and 12th-layer line meridional maxima for $\lambda = 8$ fibers of 70/30 copoly(BPDA-OTOL/BPDA-PPD), recorded as $\theta/2\theta$ scans. The relative integrated intensities of the peaks are in the ratio 12:4:1. The peak widths corrected for instrumental broadening are listed in Table 1 for the three copolymers. Plots of the squares of the observed widths against n^4 for the 80/20 ($\lambda = 5$), 70/30 ($\lambda = 8$), and 60/40 ($\lambda = 12$) fibers are shown respectively in Figures 2, 3, and 4 (curve b in each case). These plots are linear within experimental error, although in fact the raw data show the same trends as those predicted for the infinite linear chain, in that the second data point (for the 8th order) is consistently above the best straight line. The plots for the observed data have positive intercepts and are steeper than those predicted for the infinite straight chain models, suggesting that we need to consider models with finite chain lengths and/or sinuous chain conformations.

Figure 6 shows plots of δ^2 against n^4 in the $I(Z)$ data predicted for linear chain models of the 80/20 copolymer

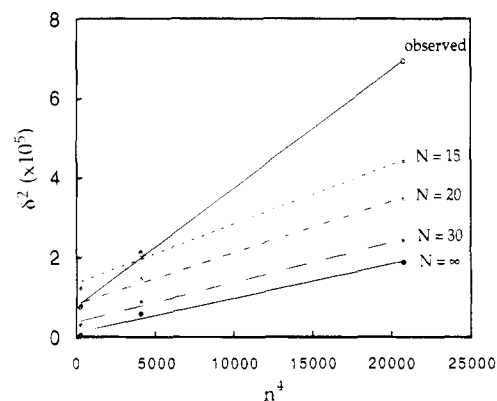


Figure 6. Plots of calculated δ^2 against n^4 for finite linear chain models of different degrees of polymerization (N) for the 80/20 copolymer. The observed data are shown for comparison.

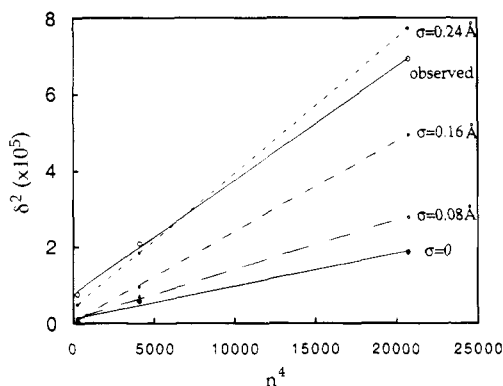


Figure 7. Plots of calculated δ^2 against n^4 for infinite chain models with different sinuosities for the 80/20 copolymer. The observed data are shown for comparison.

with different chain lengths ($N = DP$, degree of polymerization). The slopes remain approximately constant as we change the chain length (there is actually a small increase in slope with decreasing N), while the intercept moves to higher positive values. Inserting this intercept into eq 5 yields a "crystallite size" which is approximately equal to the chain length used in these models. Figure 7 shows the same kind of plots for infinite chain models with different sinuosities, as defined by the σ parameter in eq 8. The primary effect of increasing the sinuosity is to increase the slope of the plot. However, there is also a change in the intercept, which arises because the axial correlation length decreases with the introduction of sinuosity: $Q(z)$ becomes a smooth function at high z .

Thus we can match the intercept of the plot for the observed data if we use a straight chain model with a

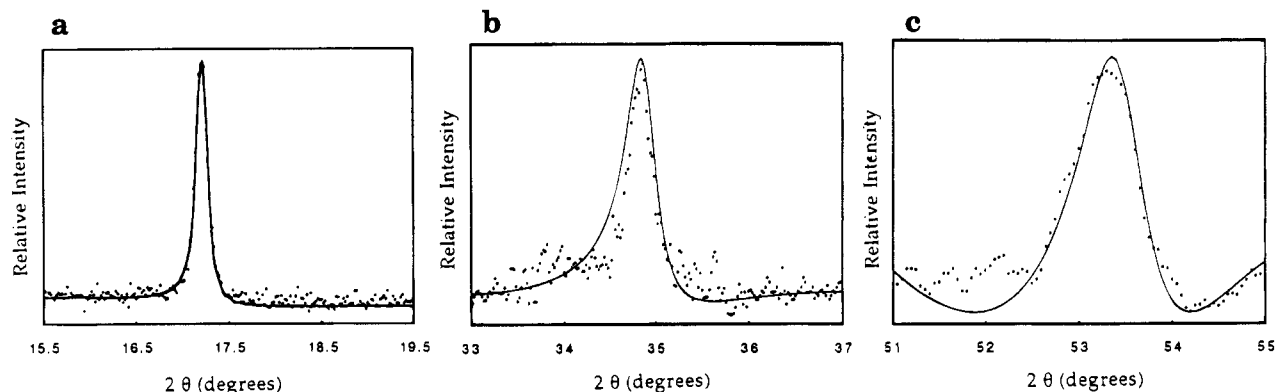


Figure 8. Plots of observed (●) and calculated (solid line) intensity against 2θ on the (a) 4th, (b) 8th, and (c) 12th layer lines for the 70/30 copolymer.

Table 2. Apparent Axial Crystallite Sizes and Corrected Axial Correlation Lengths Derived from the Meridional Line Broadening for Fibers of Copoly(BPDA-OTOL)_x(BPDA-PPD)_y

monomer ratio x/y	draw ratio λ	Scherrer crystallite size (Å) ^a	finite linear chain correlation length (Å)	finite sinuous chain	
				correlation length (Å)	sinuosity (Å) σ
100/0	2	180 ± 6	181 ± 6	183 ± 6	0.246 ± 0.002
80/20	5	360 ± 8	390 ± 10	480 ± 20	0.164 ± 0.002
70/30	8	460 ± 10	540 ± 20	800 ± 80	0.152 ± 0.003
60/40	12	470 ± 10	600 ± 40	1000 ± 150	0.133 ± 0.005
70/30	5	343 ± 7	375 ± 10	510 ± 30	0.158 ± 0.003
60/40	5	318 ± 10	355 ± 10	540 ± 35	0.148 ± 0.004

^a Based on width of 4th order.

limited chain length. Such a plot for the 80/20 copolymer is shown in Figure 2 (curve c), which is for a DP of 20, corresponding to a chain length of 390 Å. However, the slope is less than that observed, meaning that the predicted profiles for maxima on the 8th- and 12th-layer lines are too narrow. Similarly, we can match the slope of the plot for the observed data by varying the chain sinuosity, as shown in Figure 2 (curve d) with a sinuosity of $\sigma = 0.166$ Å. There is also a positive intercept at $n^4 = 0$, but it is significantly below that for the observed data. (Insertion of this intercept into eq 5 yields a "crystallite size" of ~800 Å for the model used.) However, it is possible to match *both* the intercept and slope by trial and error refinement of the chain length and sinuosity. The best fit is achieved using DP = 25 ± 1 (chain length 480 ± 20 Å) and a sinuosity $\sigma = 0.164 \pm 0.002$ Å, which corresponds to a standard deviation of $0.84 \pm 0.01\%$ in the monomer advances. The calculated plot (curve e) coincides almost exactly with curve b in Figure 2, and the predicted peak widths are listed in Table 1.

Figures 3 and 4 show the equivalent data for the 70/30 ($\lambda = 8$) and 60/40 ($\lambda = 12$) copolymers. The plots for the observed data (curve b in each case) differ from that for the 80/20 copolymer, in that the intercepts move closer to the origin and the slopes decrease with increasing PPD content; i.e., the chains become progressively more linear. However, the differences between the plots for the observed data and those predicted for the idealized infinite straight chain (curve a in each case) also diminish with increasing PPD content: the predicted 4th-, 8th-, and 12th-order peaks get broader while those observed actually sharpen. (In general, the broader the aperiodic peak predicted for the infinite chain, the less it is affected by changes in chain length and sinuosity. For example, the breadths of some of the other peaks, such as order 1–3, scarcely change until $N < 10$, and then the effect is very small.) The best fits are obtained using DP = 42 ± 4 (chain length 800

± 80 Å) and DP = 55 ± 8 (chain length 1000 ± 150 Å) for the 70/30 ($\lambda = 8$) and 60/40 ($\lambda = 12$) copolymers, respectively. The corresponding sinuosities are $\sigma = 0.152 \pm 0.003$ and 0.133 ± 0.005 Å, respectively. The progressively higher experimental errors are a consequence of the smaller broadening effects that are observed at higher PPD content. Examples of the quality of the fit obtained are seen in Figure 8, which shows plots of intensity vs 2θ for the observed and calculated 4th, 8th and 12th orders for the 70/30 ($\lambda = 8$) copolymer.

The data presented so far are for the three comonomer ratios at their maximum draw ratios. We also applied the same procedures to compare the preparation at the same draw ratio, $\lambda = 5$. Observed and calculated line widths, correlation lengths, and sinuosities for 70/30 ($\lambda = 5$) and 60/40 ($\lambda = 5$) are presented in Tables 1 and 2. It is immediately apparent that the data for the three copolymers at constant draw ratio are much more similar than those for the maximum draw ratio specimens. The raw line widths are very close, although there is a small increase with PPD content, in the same direction as predicted for the infinite linear chain. However, matching the line width by refinement of the chain lengths and sinuosities leads to essentially the same structural parameters within experimental error. Consequently, it is clear that the differences in the structure of the maximum draw ratio preparations arise simply because the presence of increasing amounts of the PPD monomer enhances the drawability.

In contrast to the striking result that the order in the chain axis direction increases with the proportion of the PPD comonomer, the lateral packing becomes progressively more disordered. However, even in the 60/40 copolymer there is significant registration, leading to off-axis Bragg reflections. Consequently, it appears that the structure contains three-dimensional ordered lamellae, separated by discontinuities or by "oriented amorphous" regions in which the chains are parallel to the

fiber axis but less well packed. Such a morphology is seen for the amorphous copoly(HBA/HNA) thermotropic copolyesters.^{15,16} The lengths of the linear segments are greater the higher the PPD content, but at the same time it is more difficult to maintain the registered lateral packing.

Table 2 gives the chain lengths for the copolymers that best match the observed data in Figures 2–4. Since only part of each observed line width is due to finite chain length, the chain lengths obtained are greater than those obtained from the observed widths using the Scherrer equation (Table 2). Use of a finite straight chain model (Table 2) also underestimates the length of the ordered regions, because it does not consider the sinuosity that is inevitable when the random sequences are packed. The latter effect is most noticeable for the 60/40 ($\lambda = 12$) copolymer, where the length of the ordered chain is increased to 1000 ± 150 Å. The correlation lengths are much higher than the axial crystallite width of 183 Å determined for the homopolymer, for which the correction for paracrystalline distortion is negligible. In separate work,¹⁷ we have measured the equivalent axial crystallite width for poly-(*p*-phenylene terephthalamide) processed as Kevlar 149 fibers and obtained a crystallite dimension of 395 Å. The correlation lengths for all three copolyimides exceed this dimension in Kevlar 149, which gives a qualitative picture of the high level of chain linearity in the copolyimide fibers.

Acknowledgment. We thank Dr. Z. Wu and Professors S. Z. D. Cheng and F. W. Harris of the University of Akron for synthesis and preparation of the fibers. This work has been supported by NSF Grant No. EEC91-

08700, the State of Ohio Department of Development, and the Edison Polymer Innovation Corporation through the Center for Molecular and Microstructure of Composites (CMMC) at Case Western Reserve University and the University of Akron.

References and Notes

- (1) Shen, D.; Wu, Z.; Liu, J.; Wang, L.; Lee, S.; Harris, F. W.; Cheng, S. Z. D.; Blackwell, J.; Wu, T.-M.; Chvalun, S. *Polym. Polym. Compos.* **1994**, *2*, 149.
- (2) Krause, S. J.; Vezie, D. L.; Adams, W. W. *Polym. Commun.* **1989**, *30*, 10.
- (3) Wu, T.-M.; Chvalun, S.; Blackwell, J.; Cheng, S. Z. D.; Wu, Z.; Harris, F. W. *Polymer*, in press.
- (4) Wu, T.-M.; Chvalun, S. N.; Blackwell, J.; Cheng, S. Z. D.; Wu, Z.; Harris, F. W. *Acta Polym.*, in press.
- (5) Harris, F. W.; Hsu, S. L. C. *High Perform. Polym.* **1989**, *1*, 1.
- (6) Takahashi, N.; Yoon, D. Y.; Parris, W. *Macromolecules* **1984**, *17*, 2583.
- (7) Kaneda, T.; Katsura, T.; Nakagawa, K.; Makino, H.; Horio, M. *J. Appl. Polym. Sci.* **1986**, *32*, 3151.
- (8) Hosemann, R.; Bagchi, S. N. *Direct Analysis of Diffraction by Matter*; North-Holland Publishing Co.: Amsterdam, 1962.
- (9) Gutierrez, G. A.; Chivers, R. A.; Blackwell, J.; Stamatoff, J. B.; Yoon, H. *Polymer* **1983**, *24*, 937.
- (10) Blackwell, J.; Gutierrez, G. A.; Chivers, R. A. *Macromolecules* **1984**, *17*, 1219.
- (11) Biswas, A.; Blackwell, J. *Macromolecules* **1987**, *20*, 2997.
- (12) Blackwell, J.; Cageao, R. A.; Biswas, A. *Macromolecules* **1987**, *20*, 667.
- (13) Blackwell, J.; Biswas, A.; Bonart, R. C. *Macromolecules* **1985**, *18*, 2126.
- (14) Chivers, R. A.; Blackwell, J.; Gutierrez, G. A. *Polymer* **1984**, *25*, 435.
- (15) Hanna, S.; Windle, A. H. *Polymer* **1988**, *29*, 207.
- (16) Hudson, S. D.; Lovinger, A. J. *Polymer* **1993**, *34*, 1123.
- (17) Wu, T.-M.; Chvalun, S. N.; Blackwell, J., in preparation.

MA950607D